Available online at www.sciencedirect.com
SCIENCE DIRECT®
Journal of Sound and Vibration 271 (2004) 297–321
JOURNAL OF SOUND AND VIBRATION
www.elsevier.com/locate/jsvi

Mobility analysis of active isolation systems

S.J. Elliott*, L. Benassi, M.J. Brennan, P. Gardonio, X. Huang

Institute of Sound and Vibration Research, University of Southampton, Southampton SO17 1BJ, UK

Received 24 September 2002; accepted 18 February 2003

Abstract

A frequency-domain formulation is used to analyze the stability and performance of an active vibration isolation system which uses feedback control. The active mount is modelled as a single-axis force actuator in parallel with a passive spring and damper. The feedback sensor measures either the absolute velocity of the equipment to be isolated at one end of the mount, or the integral of the transmitted force through the mount. The plant response, from force actuator input to sensor output, is derived for these two cases in terms of the mechanical mobilities of the two structures connected by the active mount.

The limits of the phase of the plant response are derived for the two feedback strategies and these are used to explain the stability and performance of several specific examples of active isolation systems. It is shown that, in the absence of actuator and sensor dynamics, the integrated force feedback system is unconditionally stable. The stability of the absolute velocity feedback system is, however, threatened if the vibrating base structure becomes very mobile, with a small effective mass, at the same frequency as the equipment structure becomes very stiff.

By quantifying the conditions under which velocity feedback systems can become unstable, these conditions can be avoided. If the stability of an absolute velocity feedback system can be assured, it is shown to be more effective at controlling resonances caused by equipment dynamics than integrated force feedback.

1. Introduction

This paper considers the stability and performance of active systems for the isolation of sensitive equipment from base vibration that use either absolute velocity feedback or integrated force feedback. Conventional passive isolation systems suffer from a trade-off in the choice of their damping [1]. If the passive isolator damping is too small, the equipment vibration is amplified compared with the base vibration close to the mounted natural frequency. If the passive

*Corresponding author. Tel.: +44-23-8059-2384; fax: +44-23-8059-3190.
E-mail address: sje@isvr.soton.ac.uk (S.J. Elliott).

0022-460X/$ - see front matter © 2003 Elsevier Ltd. All rights reserved.
doi:10.1016/S0022-460X(03)00770-3

isolator damping is too large, the vibration transmissibility is increased at frequencies well above the mounted natural frequency. Active isolation using skyhook damping can remove this trade-off [2]; controlling the vibration amplification and thus reducing the motion of the equipment at the mounted natural frequency, while not degrading the high frequency vibration isolation.

Absolute velocity feedback is sometimes referred to as skyhook damping [2], although its action is not completely equivalent unless the active force reacts off a rigid base structure [3]. The absolute velocity signal can conveniently be derived by integrating the output of an inertial accelerometer.

Integrated force feedback [4] has a similar effect to skyhook damping [5], but has the advantage of being stable for a wider range of systems to which it is attached [6]. If the equipment being isolated is also very heavy and the vibration levels are very low, such as in space applications, it may also be considerably easier to measure the force transmitted to the equipment rather than its velocity [5]. In more industrial applications, however, the required force gauge may be too fragile for practical use. The vibration reduction may also not be as great as with absolute velocity feedback.

In Section 2 the plant responses, from actuator input to sensor output, of the open loop systems with either absolute velocity feedback or integrated force feedback are derived in terms of the mechanical impedance of the mount and the input mobilities of the equipment and base structure. This analysis is similar to that of Blackwood and von Flotow [7]. The frequency responses of these plant responses are then analyzed in the general case to show that the integrated force feedback system is unconditionally stable, whatever the equipment and base dynamics, although under certain circumstances it may not be robust to actuator and sensor dynamics, whereas no such general proof of stability can be derived for the absolute velocity feedback system.

In Section 3 the particular case is analyzed of when the base structure is rigid. It is shown that not only is absolute velocity feedback unconditionally stable under these conditions, but that the plant response is then passive and so the feedback system has a guaranteed 90° phase margin. The integrated force feedback system is unconditionally stable, but has a phase margin which can become small under certain conditions. The frequency response, Nyquist plot and root locus diagrams are discussed, with either absolute velocity feedback or integrated force feedback, for a particular case in which the equipment is dynamic.

In Section 4 another special case is analyzed; when the base structure is a mass. In this case an absolute velocity feedback system can become unstable under certain conditions. This is illustrated using the example isolation system discussed by Preumont et al. [6]. The conditions for instability in this case are analyzed in some detail.

Finally, in Section 5 the case of a flexible base structure and a flexible equipment structure is considered. In the particular example analyzed, which is regarded as being reasonably representative of an equipment isolation system, absolute velocity control is again unconditionally stable, despite worst-case conditions for the phase of the base mobility and equipment mobility occurring in the same frequency range.

2. General analysis

The general arrangement assumed for the active isolation problem is shown in Fig. 1, in which the equipment structure is isolated from the vibrating base structure by a single-axis active mount,

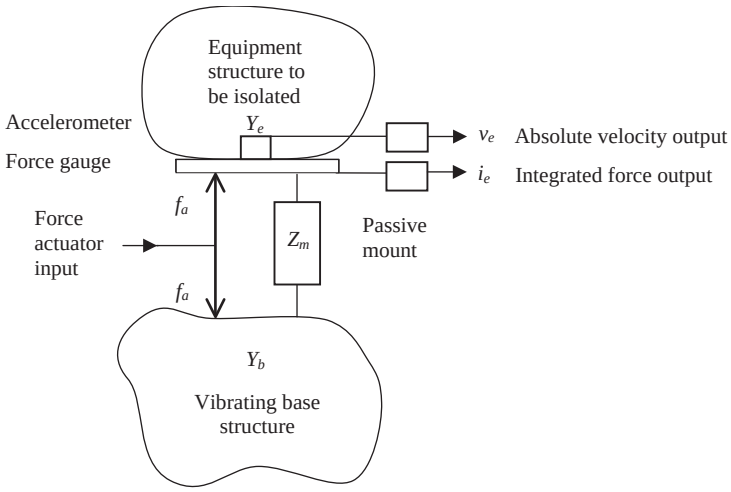

Fig. 1. Schematic diagram used to derive the plant response from a force actuator to absolute velocity or integrated force sensor.

represented by its Thévenin equivalent. The objective of the first part of the general analysis is to derive the plant responses from the actuator force input, f_a, to either the absolute velocity output on the equipment, v_e, or the integrated force output, i_e, which is the integral of the force transmitted to the equipment, f_e. These plant responses will then be used to deduce the conditions under which a fixed-gain feedback loop, from either the absolute velocity or integrated force sensor to the force actuator, will be stable. The analysis will initially be undertaken in the Laplace domain, in terms of the mobilities of the equipment and base structures, Y_e and Y_b, and the impedance of the mount, Z_m, although the explicit dependence of the variables on the Laplace variable, s, is suppressed unless it is required. The frequency response is derived when required by setting $s = \mathrm{j}\omega$.

2.1. Derivation of plant responses

If the velocity of the equipment at the point of attachment is v_e and the force transmitted by the actuator and the mount is f_e, the equipment (or clean body) dynamics are defined by its input, or point, mobility

$$\frac{v_e}{f_e} = Y_e. \tag{1}$$

Similarly if the velocity of the base at the point of attachment is v_b and the force transmitted by the actuator and mount is f_b, the base (or dirty body) dynamics are defined by its input mobility

$$\frac{v_b}{f_b} = Y_b. \tag{2}$$

The mount dynamics are defined to include both the effect of any passive mount and the passive response of the actuator, both of which are assumed to have negligible mass, so that the mount

dynamics are defined by its mechanical impedance

$$\frac{f_m}{v_m} = Z_m, \tag{3}$$

where f_m is the force acting through the mount and v_m is the difference in velocity between its two ends.

The total force acting on the equipment structure is thus

$$f_e = f_a + Z_m(v_b - v_e), \tag{4}$$

where all forces and velocities are assumed to act in the same direction, so that the total force acting on the base is $f_b = -f_e$. Using this and Eqs. (1) and (2), the total force on the equipment structure can be written as

$$f_e = f_a - Z_m(Y_b + Y_e)f_e, \tag{5}$$

so that

$$\frac{f_e}{f_a} = \frac{1}{1 + Z_m(Y_b + Y_e)}. \tag{6}$$

The absolute velocity of the equipment is related to the force acting on it by the equation $v_e = Y_e\ f_e$, so the plant response from actuator force to absolute equipment velocity can be written in the Laplace domain as

$$G_v(s) = \frac{v_e(s)}{f_a(s)} = \frac{Y_e(s)}{1 + Z_m(s)(Y_b(s) + Y_e(s))}. \tag{7}$$

Also, if $i_e(s) = f_e(s)/s$ is the integrated force acting on the equipment, then the plant response from actuator force to this output signal in the Laplace domain is

$$G_i(s) = \frac{i_e(s)}{f_a(s)} = \frac{1/s}{1 + Z_m(s)(Y_b(s) + Y_e(s))}. \tag{8}$$

If the equipment structure behaved entirely like a rigid body of mass, m_e, its input mobility would be equal to $Y_e(s) = 1/(sm_e)$. The plant response from actuator force to absolute velocity then becomes proportional to that from actuator force to integrated force, and the two control strategies would behave identically. In general, however, the equipment structure will be dynamic and its input mobility will have a more complicated form than that above, in which case the behaviour of the control system is significantly different if the feedback signal is either absolute velocity or integrated force.

2.2. Frequency response conditions on stability

Since the mount is assumed to have a negligible mass, then without loss of generality its impedance can be written as

$$Z_m = \frac{k_m}{s} + c_m, \tag{9}$$

where k_m is the mount's stiffness and c_m its damping factor, both of which may be frequency dependent. Some rather general conditions on stability can be derived by examining the reciprocal

of the plant frequency response. In the case of absolute velocity feedback, Eq. (7), this is equal to

$$G_v^{-1}(\mathrm{j}\omega) = Y_e^{-1}(\mathrm{j}\omega)\ [1 + Z_m(\mathrm{j}\omega)(Y_b(\mathrm{j}\omega) + Y_e(\mathrm{j}\omega))]. \tag{10}$$

The first term in this expression, $Y_e^{-1}(\mathrm{j}\omega)$, is passive, since $Y_e(\mathrm{j}\omega)$ is an input mobility, and thus has a phase shift of between –90° and 90°. The phase shift of $Z_m(\mathrm{j}\omega)$ will be $-90°$ if the mount is dominated by its stiffness, reducing to 0° if it is dominated by its damping. The phase shift of $Y_b(\mathrm{j}\omega) + Y_e(\mathrm{j}\omega)$ is between –90° and 90°, since both $Y_b(\mathrm{j}\omega)$ and $Y_e(\mathrm{j}\omega)$ are passive input mobilities.

The phase shift of $Z_m(\mathrm{j}\omega)(Y_b(\mathrm{j}\omega) + Y_e(\mathrm{j}\omega))$, and thus $1 + Z_m(\mathrm{j}\omega)(Y_b(\mathrm{j}\omega) + Y_e(\mathrm{j}\omega))$, can therefore potentially vary between $-180°$ and 90°, and the overall phase shift of $G_v^{-1}(\mathrm{j}\omega)$ could range between $-270°$ to $+180°$. The phase limitations on the plant response from actuator force to absolute equipment velocity are, in general, thus given by

$$-180° < \angle\, G_v(\mathrm{j}\omega) < 270°, \tag{11}$$

and in the most general case a constant gain feedback loop is only conditionally stable. It has previously been shown by Serrand [8] that if the equipment remains rigid and has a mass-like mobility, then the phase of G_v is restricted to $-180° < \angle\, G_v(\mathrm{j}\omega) < 90°$, and the system is unconditionally stable. Sciulli and Inman [9] have also discussed the design of passive and active isolators for this kind of flexible base, rigid equipment isolation problem. In this section we assume that the equipment may also be flexible and seek a more general condition to guarantee the stability of the feedback system.

The plant G_v, with a constant feedback gain, can only become unstable if the phase shift of $G_v(\mathrm{j}\omega)$ were greater than 180°. The conditions for this to occur can be examined by returning to the general expression for $G_v^{-1}(\mathrm{j}\omega)$ in Eq. (10), which must have a phase shift of less than $-180°$ for the feedback system to be unstable. The phase of $G_v^{-1}(\mathrm{j}\omega)$ cannot be less than $-180°$ unless the phase shift of $Y_e^{-1}(\mathrm{j}\omega)$ is negative, i.e., the equipment mobility is stiffness-controlled. In order to derive a relatively simple condition for stability we will assume that the damping in the system can be neglected and so all the impedances and mobilities are purely reactive. The stiffness-controlled equipment mobility can thus be written as

$$Y_e(\mathrm{j}\omega) = \frac{\mathrm{j}\omega}{k_e}, \tag{12}$$

where k_e is the dynamic stiffness of the equipment, which in general is frequency dependent.

In order for the phase of $[1 + Z_m(\mathrm{j}\omega)(Y_e(\mathrm{j}\omega) + Y_b(\mathrm{j}\omega))]$ in Eq. (10) to be less than $-90°$ overall, and thus the phase shift of $G_v^{-1}(\mathrm{j}\omega)$ to be sufficiently negative for the feedback system to be unstable, then the real part of $[1 + Z_m(\mathrm{j}\omega)(Y_e(\mathrm{j}\omega) + Y_b(\mathrm{j}\omega))]$ must be negative, so that

$$Re[Z_m(\mathrm{j}\omega)(Y_e(\mathrm{j}\omega) + Y_b(\mathrm{j}\omega))] < -1. \tag{13}$$

If the damping in the mount is small, then to a good approximation we may take

$$Z_m(\mathrm{j}\omega) = \frac{k_m}{\mathrm{j}\omega}, \tag{14}$$

where k_m is the stiffness of the mount, and using Eq. (12) for $Y_e(\mathrm{j}\omega)$, then

$$Z_m(\mathrm{j}\omega)(Y_e(\mathrm{j}\omega) + Y_b(\mathrm{j}\omega)) = \frac{k_m}{k_e} + \frac{k_m}{\mathrm{j}\omega} Y_b(\mathrm{j}\omega). \tag{15}$$

The only way in which the real part of Eq. (15) can be less than –1, is if the mobility of the base is mass-dominated, so that

$$Y_b(\mathrm{j}\omega) = \frac{1}{\mathrm{j}\omega m_b}, \tag{16}$$

where m_b is the effective mass of the base structure, which in general is frequency dependent. In this case

$$Z_m(\mathrm{j}\omega)(Y_e(\mathrm{j}\omega) + Y_b(\mathrm{j}\omega)) = \frac{k_m}{k_e} - \frac{k_m}{\omega^2 m_b}. \tag{17}$$

The condition under which instability may occur, Eq. (13), then becomes

$$\frac{k_m}{k_e} - \frac{k_m}{\omega^2 m_b} < -1, \tag{18}$$

so that

$$\frac{k_t}{\omega^2 m_b} > 1, \tag{19}$$

where

$$k_t = \frac{k_m k_e}{(k_m + k_e)}, \tag{20}$$

is the total stiffness of the mount and equipment, as experienced by the base structure. The parameter $k_t/\omega^2 m_b$, which must always be less than unity if the system is to be unconditionally stable, is equal to the modulus of the mobility of the base divided by the mobility of the mount and equipment, under the conditions that the equipment is stiffness-controlled and the base is mass-controlled.

In summary then, a feedback system from absolute equipment velocity to actuator force will be unconditionally stable unless every one of the following conditions is simultaneously satisfied at some frequency:

(1) The equipment dynamics are stiffness-dominated, so that $Y_e(\mathrm{j}\omega) = \mathrm{j}\omega/k_e$ and $k_e > 0$,
(2) the base dynamics are mass-dominated, so that $Y_b(\mathrm{j}\omega) = 1/\mathrm{j}\omega m_b$ and $m_b > 0$ and
(3) the stability parameter is greater than unity; $k_t/\omega^2 m_b > 1$, where $k_t = k_m k_e/(k_m + k_e)$.

Turning now to the reciprocal frequency response of the plant in the case of integrated force feedback, this can be written, from Eq. (8), as

$$G_i^{-1}(\mathrm{j}\omega) = \mathrm{j}\omega + \mathrm{j}\omega\ Z_m(\mathrm{j}\omega)(Y_b(\mathrm{j}\omega) + Y_e(\mathrm{j}\omega)), \tag{21}$$

and using Eq. (9) for Z_m,

$$G_i^{-1}(\mathrm{j}\omega) = \mathrm{j}\omega + (k_m + \mathrm{j}\omega c_m)(Y_b(\mathrm{j}\omega) + Y_e(\mathrm{j}\omega)). \tag{22}$$

The phase shift of $(Y_b(\mathrm{j}\omega) + Y_e(\mathrm{j}\omega))$ is between $\pm 90^\circ$, since both $Y_b(\mathrm{j}\omega)$ and $Y_e(\mathrm{j}\omega)$ are passive, whereas the term $(k_m + \mathrm{j}\omega c_m)$ can potentially have a phase shift of between 0° and 90°. Consequently the overall phase shift of $G_i^{-1}(\mathrm{j}\omega)$ can never be greater than 180° and so $G_i(\mathrm{j}\omega)$ can

never have a phase shift of less than -180°. The limitations on the phase of $G_i(j\omega)$ are thus

$$-180^\circ < \angle G_i(j\omega) < 90^\circ. \tag{23}$$

In the absence of actuator or sensor dynamics, and assuming that the mount has negligible mass, the integrated force feedback control system is thus unconditionally stable for any combination of base and equipment dynamics.

This control system is even more robustly stable if the active mount is stiff. If $k_m \gg \omega c_m$, then $G_i(j\omega)$ has a phase shift of only $\pm 90^\circ$ and is thus completely passive. Its Nyquist plot is then entirely on the right-hand side of the imaginary axis and the feedback system has an infinite gain margin and a phase margin of at least 90°. This particularly attractive situation occurs, for example, when a "hard mount" such as a piezoceramic actuator is used, in which case $k_m \gg \omega c_m$ up to a very high frequency. At these high frequencies the $j\omega$ term on the right-hand side of Eq. (22) will dominate the other terms and so $G_i^{-1}(j\omega)$ will be large. $G_i(j\omega)$ will thus generally be close to the origin at such high frequencies and there is little danger of unmodelled actuator dynamics destabilising the system in this case.

In the following sections the consequences of making different assumptions about the dynamics of the base structure are explored for the practical stability of both absolute velocity and integrated force feedback systems.

3. Case of a rigid base structure

3.1. Absolute velocity feedback

The base structure is assumed to be rigid, so that

$$Y_b(j\omega) = 0, \tag{24}$$

but has an imposed velocity of v_b.

Under these conditions the frequency response of the plant with an absolute velocity sensor, Eq. (7), becomes

$$G_v(j\omega) = \frac{Y_e(j\omega)}{1 + Y_e(j\omega)\ Z_m(j\omega)}, \tag{25}$$

so that its reciprocal is

$$G_v^{-1}(j\omega) = Y_e^{-1}(j\omega) + Z_m(j\omega), \tag{26}$$

which is the sum of the input impedance of the equipment and the impedance of the mount. Both terms in Eq. (26) are passive, with phase shifts of between $\pm 90^\circ$, and so $G_v(j\omega)$ also has a phase shift of between $\pm 90^\circ$. Its Nyquist plot is thus guaranteed to be on the right side of the imaginary axis and so a feedback system with absolute velocity feedback with a rigid base is unconditionally stable with an infinite gain margin and a phase margin of at least 90°. This condition will also be closely approximated when $Y_b(j\omega) \ll Y_e(j\omega)$, i.e., the base is much less mobile than the equipment. In terrestrial applications, when the base is the ground, this approximation is often valid.

As an example of such a system, the plant response for the isolation system shown in Fig. 2 has been calculated. The dynamic equipment structure has been modelled by a main mass, m_e, of

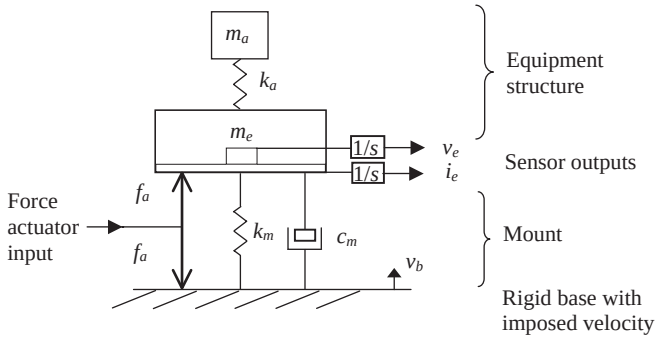

Fig. 2. An example of an active isolation system with a rigid base and dynamic equipment structure.

1.7 kg with an appendage consisting of an additional mass, m_a, of 0.5 kg attached to the main mass by a spring of stiffness, k_a, equal to 12,000 N m^{-1}. The mobility of the equipment in this case is given by

$$Y_e = (Z_i + Z_a)^{-1}, \tag{27}$$

where Z_i is the inertial impedance of the equipment,

$$Z_i(s) = s\ m_e, \tag{28}$$

and Z_a is the impedance of the appendage,

$$Z_a(s) = \frac{sm_a k_a}{k_a + s^2 m_a}. \tag{29}$$

The mount is assumed to also have a stiffness, k_m, of 12,000 N m^{-1} and a damping factor, c_m, of 33 N s m^{-1} and rests on a rigid base.

The frequency response of the plant response from actuator force to absolute equipment velocity is shown in Fig. 3(a) and its Nyquist plot is shown in Fig. 3(b). The Nyquist plot is the locus of the real and imaginary parts of $GH(j\omega)$, where H is the real feedback gain in this case and $G(j\omega)$ is the plant's frequency response, as ω varies from zero to infinity. If the mirror image response, as ω varies from minus infinity to zero, is added, which is the complex conjugate of that above, the system is stable in this case, provided the locus does not enclose the Nyquist point $(-1,0)$ [10]. The system has a mount-dominated resonance at about 11 Hz, in which m_e and m_a are moving in phase on the mount stiffness k_m, so that the resonant frequency is approximately equal to

$$f_m = \frac{1}{2\pi}\sqrt{\frac{k_m}{m_a + m_e}}. \tag{30}$$

The damping ratio of this resonance is about 10%.

The antiresonance in the frequency response, at about 25 Hz, is due to the attachment acting as a tuned vibration neutraliser at a frequency given by

$$f_a = \frac{1}{2\pi}\sqrt{\frac{k_a}{m_a}}, \tag{31}$$

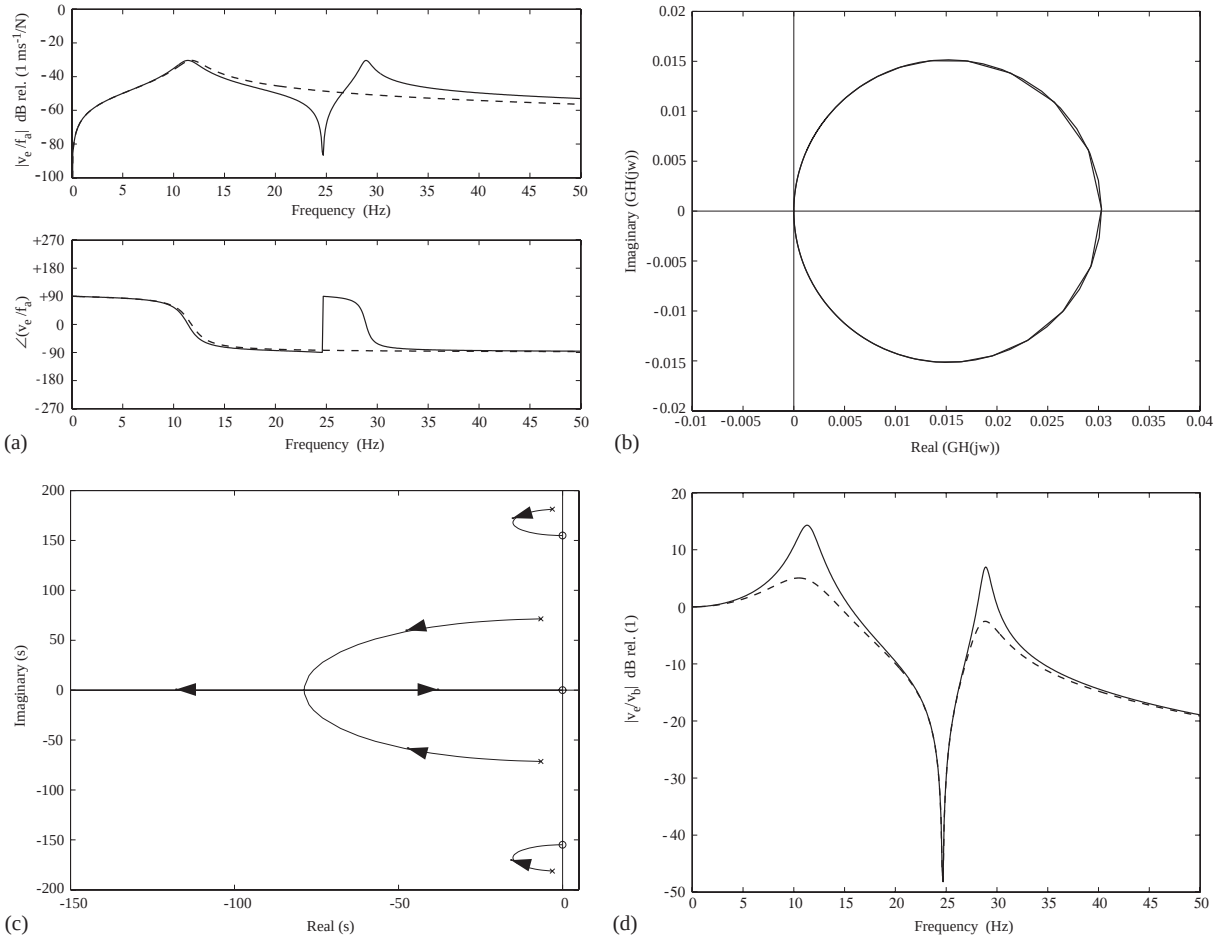

Fig. 3. (a) Frequency response of the plant response from actuator force to absolute equipment velocity for the isolation system on a rigid base shown in Fig. 2 (solid line) and with the equipment dynamics suppressed by setting $k_a = \infty$ (dashed line). (b) Nyquist plot of the plant response from actuator force to absolute equipment velocity for the system shown in Fig. 2. (c) Root locus diagram for the plant response from actuator force to absolute equipment velocity for the system shown in Fig. 2. (d) Open and closed loop transmissibilities from the base velocity, v_b, to the equipment velocity, v_e, for a feedback system in which absolute equipment velocity is fed back to the actuator for the isolator on a rigid base as in Fig. 2.

at which frequency the input impedance of the attachment, Z_a in Eq. (29), is infinite and this prevents the equipment main mass from moving.

The second resonance in the frequency response, at about 29 Hz, is dominated by the main equipment mass and attached mass resonating on the stiffness of the attachment, so that the main equipment mass and the attached mass move out of phase, at a frequency slightly higher than.

$$f_e = \frac{1}{2\pi}\sqrt{\frac{k_a(m_a + m_e)}{m_a m_e}}. \tag{32}$$

The plant response with the equipment dynamics suppressed, by setting $k_a = \infty$, is shown as the dashed curve in Fig. 3(a), which confirms that the antiresonance and higher frequency resonance are due to the equipment dynamics. The antiresonance, with its associated phase increase of 180°, occurs between the two resonances, and so the phase is maintained between $\pm 90°$, as expected. The magnitudes of the two resonant peaks are the same in this case, since no damping is assumed in the attachment, so that the two circles in the Nyquist plot coincide. The Nyquist plot is entirely on the right-hand side of the real axis because the phase shift in the plant is never greater than $\pm 90°$, so that the control system is very robust with an infinite gain margin and a phase margin of at least 90°. This control system would thus remain stable even if low frequency phase shifts, due to transducer conditioning electronics, and high frequency phase shifts, due to actuator limitations, were introduced [11,12].

The root locus plot for this system is shown in Fig. 3(c), with damped pairs of poles at the two resonant frequencies and zeros at the origin and at the antiresonance. This diagram represents the locus of the poles of the closed loop feedback system as the feedback gain is increased from zero to infinity [10]. The alternating pole-zero pattern prevents phase accumulation. The poles remain in the left-hand side of the s plane for all feedback gains confirming that the system is unconditionally stable.

The performance of the feedback system is shown in Fig. 3(d) in terms of the open and closed loop transmissibilities, i.e., the ratio of the equipment velocity to an imposed base velocity. The feedback gain has been chosen such that the phase margin of the system is 120°. Even with this very robust feedback controller, reductions of more than 10 dB have been obtained at both the base-dominated resonance and equipment-dominated resonance.

3.2. Integrated force feedback

When the base is rigid, the reciprocal frequency response of the plant with integrated force feedback becomes

$$G_i^{-1} = \mathrm{j}\omega(1 + Y_e(\mathrm{j}\omega)Z_m(\mathrm{j}\omega)). \tag{33}$$

Writing the mount impedance in terms of its stiffness and damping components, as in Eq. (9), this can be written as

$$G_i^{-1} = \mathrm{j}\omega + k_m Y_e(\mathrm{j}\omega) + \mathrm{j}\omega c_m Y_e(\mathrm{j}\omega). \tag{34}$$

If the mount has significant damping and the equipment is stiffness-controlled, so that the phase of $Y_e(\mathrm{j}\omega)$ is about 90°, then the third term in Eq. (34) could be large and have a phase shift of 180°. The Nyquist plot of $G_i(\mathrm{j}\omega)$ could thus approach the real axis in the third quadrant and any additional phase lag, due to actuator dynamics for example, could destabilize the system [11,12].

The frequency response of the plant from actuator force to integrated force acting on the equipment is shown in Fig. 4(a) for the case shown in Fig. 2 and with the parameters noted above. The corresponding plant response with $k_a = \infty$, i.e., with the equipment dynamics suppressed, is shown in the dashed curves from which it can again be seen that the equipment dynamics account for the upper resonance.

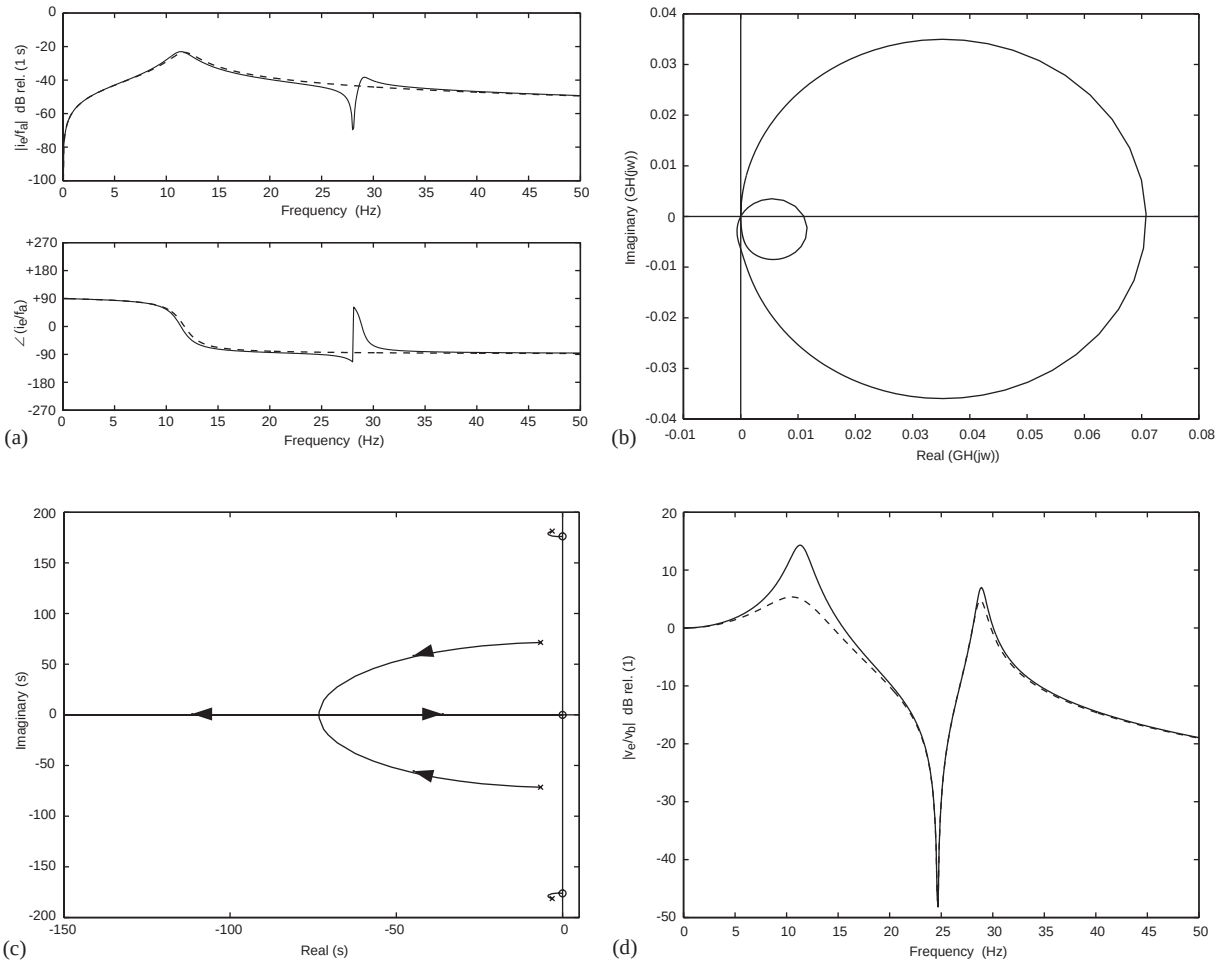

Fig. 4. (a) Frequency response of the plant from actuator force to integrated equipment force for the isolation system on a rigid base shown in Fig. 2 (solid line) and with the equipment dynamics suppressed by setting $k_a = \infty$ (dashed line). (b) Nyquist plot of the plant from actuator force to integrated equipment force for the isolation system on a rigid base shown in Fig. 2. (c) Root locus design for the plant from actuator force to integrated equipment force for the isolation system on a rigid base shown in Fig. 2. (d) Open and closed loop transmissibilities from the base velocity, v_b, to the equipment velocity, v_e, for a feedback system in which the integrated equipment force is fed back to the actuator for the isolator on a rigid base as in Fig. 2.

The frequencies of the two resonances are the same as those in the plant response above with absolute velocity feedback. The frequency of the antiresonance has increased so that it is very close to that of the second resonance. The frequency of the antiresonance is now given by the frequency at which the equipment structure's mobility becomes infinite, i.e.,

$$f_z = \frac{1}{2\pi}\sqrt{\frac{k_a(m_a + m_e)}{m_a m_e}}. \tag{35}$$

The second resonance has a smaller magnitude than the first in this case and so forms a smaller loop in the Nyquist plot, as shown in Fig. 4(b). The phase shift falls below -90° just before the antiresonance, so that the Nyquist plot strays into the third quadrant and the plant is no longer passive.

The root locus diagram for this case is shown in Fig. 4(c), and because the zero is now very close to the pole associated with the second resonance, the corresponding loop of the root locus into the left-hand side of the s plane is smaller than in the case of velocity feedback and so less damping can be achieved at these frequencies.

The velocity transmissibility from base to main equipment mass is shown in Fig. 4(d) without control and with the integrated force feedback loop. The maximum gain has again been adjusted so that the system would be stable if an additional phase lag of 120° was introduced and is thus comparable with that shown for the velocity feedback in Fig. 3(d). There is a similar attenuation in the first, mount-dominated, resonance, about 10 dB, but force feedback gives clearly a smaller attenuation of the second peak, about 2 dB, than velocity feedback.

4. Case of a mass-controlled base structure

In some classes of application, such as in space when the base structure is a satellite, the base structure will have a mass-controlled dynamic behaviour at low frequencies. The input mobility of the base is then equal to

$$Y_b = \frac{1}{sm_b}, \tag{36}$$

where m_b is the effective mass of the base structure.

In order to perform some illustrative simulations we will continue to assume that the equipment consists of a main mass m_e with an additional mass of m_a attached to it via a spring of stiffness k_a, as studied by Preumont et al. [6], so that the system is as illustrated in Fig. 5.

4.1. Absolute velocity feedback

We begin the discussion with the case of absolute velocity feedback and with the additional mass attached to the equipment, m_a, being 0.5 kg. The other parameters are $m_e = 1.7$ kg,

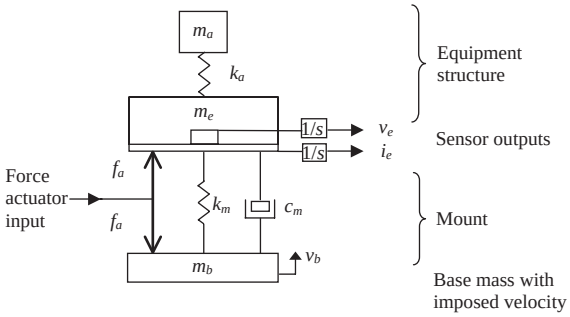

Fig. 5. An example of an isolation system with a mass-controlled base structure.

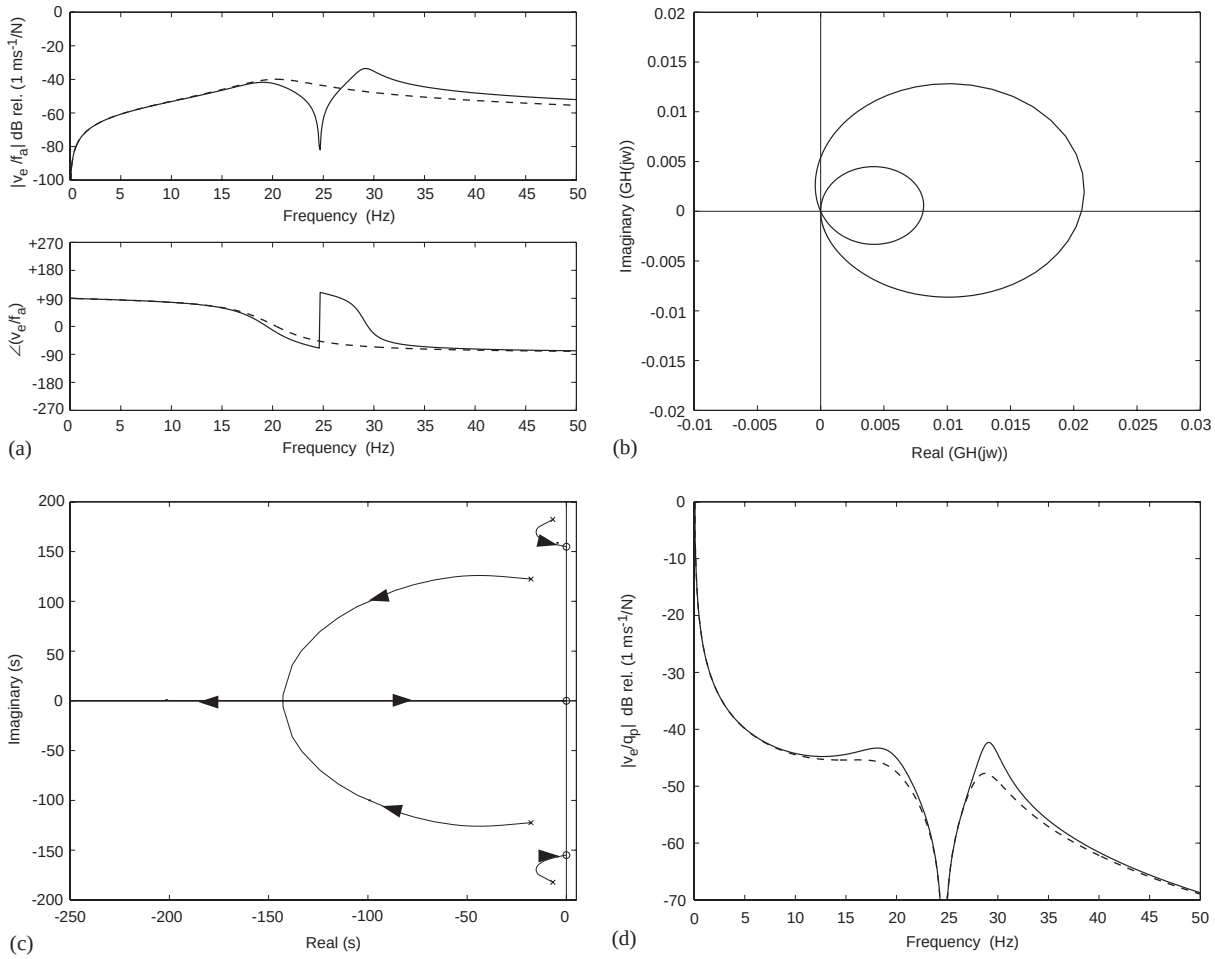

Fig. 6. (a) Frequency response of the plant response from actuator force to absolute equipment velocity for the system shown in Fig. 5 with $m_a = 0.5\,\mathrm{kg}$ (solid line) and with the equipment dynamics suppressed by setting $k_a = \infty$ (dashed line). (b) Nyquist plot of the plant response from actuator force to absolute equipment velocity for the system shown in Fig. 5 with $m_e = 0.5\,\mathrm{kg}$. (c) Root locus plot of the feedback system with the plant response from actuator force to absolute equipment velocity for the system shown in Fig. 5 with $m_e = 0.5\,\mathrm{kg}$. (d) Open and closed loop responses from a force on the base structure to absolute equipment velocity for the system shown in Fig. 5 with absolute velocity feedback and $m_e = 0.5\,\mathrm{kg}$.

$m_b = 1.1\,\mathrm{kg}$, $k_a = 12,000\,\mathrm{N\,m^{-1}}$, $k_m = 12,000\,\mathrm{N\,m^{-1}}$ and $c_m = 33\,\mathrm{N\,s\,m^{-1}}$. The frequency response of the plant in this case is shown in Fig. 6(a).

The first peak in the response, at about 20 Hz, has an undamped natural frequency of about

$$f_m = \frac{1}{2\pi}\sqrt{\frac{k_m}{m_1}}, \tag{37}$$

where

$$m_1 = \frac{m_b(m_e + m_a)}{m_b + m_e + m_a}, \tag{38}$$

and is primarily due to the mass of the base and the total mass of the equipment resonating on the mount stiffness. The zero in the plant response again occurs at the natural frequency of the attachment

$$f_a = \frac{1}{2\pi}\sqrt{\frac{k_a}{m_a}}, \tag{39}$$

at which frequency the attachment acts like a vibration neutraliser with a very high impedance that pins the equipment structure. The second peak in Fig. 6(a), at about 29 Hz, has an undamped natural frequency of about

$$f_e = \frac{1}{2\pi}\sqrt{\frac{k_a}{m_2}}, \tag{40}$$

where

$$m_2 = \frac{m_a\,(m_e + m_b)}{(m_e + m_b + m_a)}, \tag{41}$$

and is primarily due to the attached mass of the equipment reacting off the combination of the main equipment mass and the base mass and resonating on the stiffness of the attachment.

The Nyquist plot and root locus diagram are shown for this case in Figs. 6(b) and (c), from which it can be seen that absolute velocity feedback is unconditionally stable, although the phase does increase beyond 90° just after the resonance, causing the Nyquist plot to move into the second quadrant as predicted by Eq. (10). Thus although the system does have an alternating pole-zero structure, it is not passive. The open and closed loop velocity response on the equipment due to a force on the base mass are shown in Fig. 6(d), with the feedback gain again adjusted so that the phase margin is again 120°. In this case the first resonance has been attenuated by about 3 dB and the second by about 5 dB.

If, however, the mass of the attachment to the equipment is increased to 3.5 kg [6], for which the plant response is shown in Fig. 7(a), the resonance frequency of the equipment, f_e at about 12 Hz, is now below that of the basic mounted natural frequency, f_m at about 25 Hz. The antiresonance, which always occurs below the equipment resonance frequency, is now below both of the two resonance frequencies of the system and the phase lead due to this antiresonance causes the phase to increase to about 270° before falling through to 90° after the first resonance and −90° after the second resonance, as shown in Fig. 7(a). The plant response with the equipment dynamics suppressed by setting $k_a = \infty$ is shown as the dashed line in Fig. 7(a) and does not show the phase advance beyond 90°. The Nyquist plot shown in Fig. 7(b) shows that the equipment resonance, which now has a phase that goes from about +270° to +90°, causes a loop on the left-hand side of the imaginary axis. The feedback control system is thus only conditionally stable, as confirmed by the root locus diagram shown in Fig. 7(c). The open and closed loop velocity response on the equipment due to a force on the base mass is shown in Fig. 7(d), when the feedback gain is close to

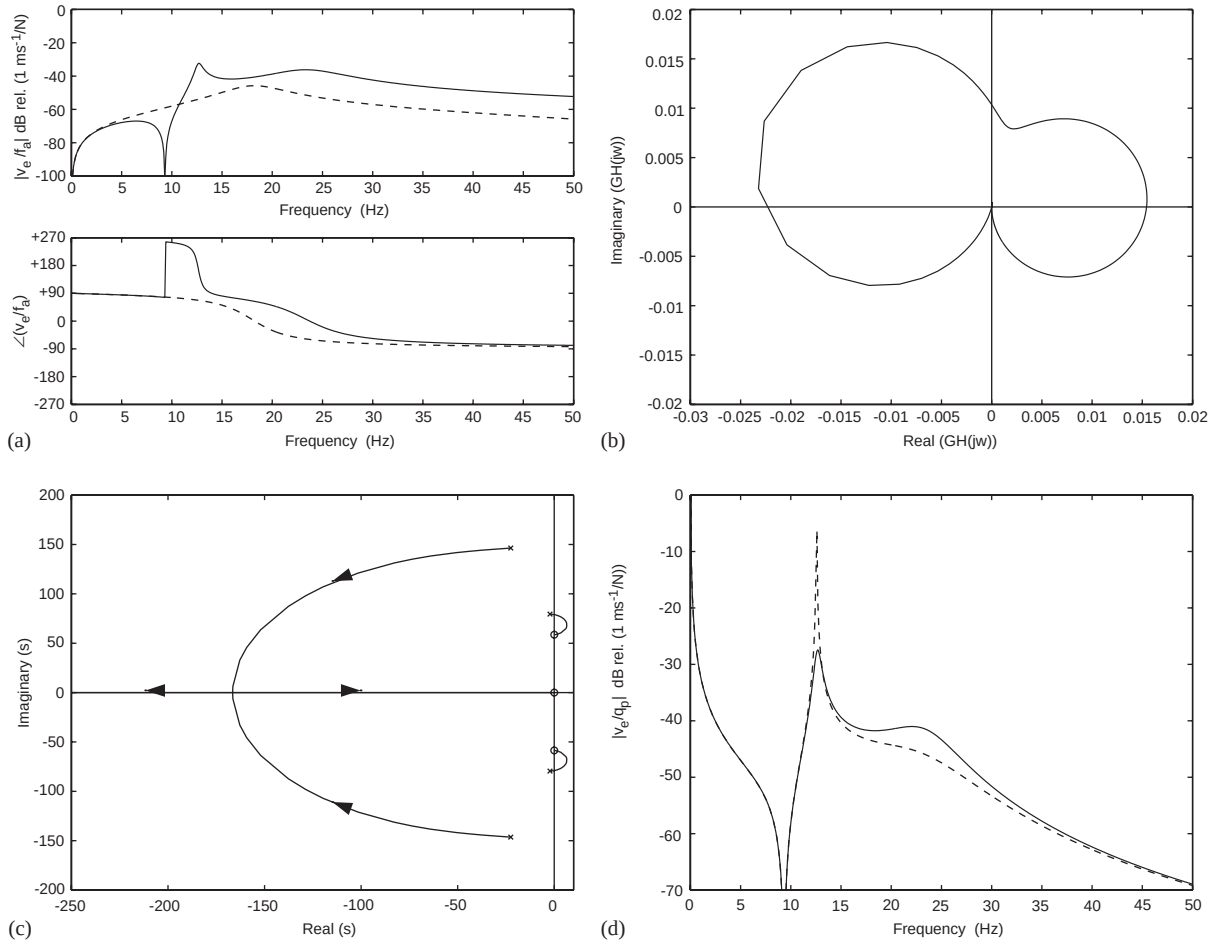

Fig. 7. (a) Frequency response of the plant from actuator force to absolute equipment velocity for the system shown in Fig. 5 with $m_a = 3.5\,\text{kg}$ (solid line) and with the equipment dynamics suppressed by setting $k_a = \infty$ (dashed line). (b) Nyquist plot of the plant response from actuator force to absolute equipment velocity for the system shown in Fig. 5 with $m_a = 3.5\,\text{kg}$. (c) Root locus diagram of the feedback control system with the plant from actuator force to absolute equipment velocity for the system shown in Fig. 5 with $m_a = 3.5\,\text{kg}$. (d) Open and closed loop responses from a force on the base structure to the equipment velocity for the system shown in Fig. 5 with absolute velocity feedback and $m_a = 3.5\,\text{kg}$.

the maximum before instability. Some attenuation at the mount resonance is achieved but this is now accompanied by enhancement of the velocity at the equipment resonance.

This change in stability behaviour with the mass of the attachment can be understood in terms of the stability conditions listed at the end of Section 2. The base dynamics are always mass-dominated in this case, with m_b being equal to 1.1 kg. The equipment dynamics are stiffness-dominated in the frequency range between the zero in the plant response caused by the attachment resonance, and the next resonance, which is also due to the dynamics of the equipment. If $m_a = 0.5\,\text{kg}$ this frequency range is from about 25–29 Hz, and if $m_a = 3.5\,\text{kg}$ this frequency range

is from about 9–13 Hz. In either case the dynamic stiffness of the equipment at the lower end of this frequency range is large, i.e., $k_e \gg k_a$. The total stiffness, k_t, defined to be $k_m k_e/(k_m + k_e)$ in Eq. (20), is thus approximately equal to k_m, i.e., about 12,000 N m^{-1}.

The third condition for the system to be only conditionally stable is that $k_t/\omega^2 m_b > 1$, Eq. (19), which will be most stringent for the lowest frequency at which both the base is mass-controlled and the equipment is stiffness-controlled, i.e., 25 Hz if $m_a = 0.5$ kg and 9 Hz if $m_a = 3.5$ kg. Substituting these values into Eq. (19) we find

$$\frac{k_t}{\omega^2 m_b} = 0.44 \quad \text{if} \quad m_a = 0.5\,\text{kg}, \tag{42}$$

i.e., the system is predicted to be unconditionally stable, as observed, and

$$\frac{k_t}{\omega^2 m_b} = 3.41 \quad \text{if} \quad m_a = 3.5\,\text{kg}, \tag{43}$$

i.e., the system is predicted to be only conditionally stable, again as observed in the simulations. The maximum value that the attached equipment mass can take before the system becomes conditionally stable can be estimated from the fact that the lowest frequency at which the equipment is stiffness-controlled is given by $\sqrt{k_a/m_a}$. Also using the fact that at this frequency $k_e \gg k_m$ so that $k_t = k_m$, the system will become conditionally stable when

$$\frac{k_m}{\omega_a^2 m_b} > 1, \quad \text{i.e.,} \quad \frac{k_m m_a}{k_a m_b} > 1. \tag{44}$$

In the case considered here $k_m = k_a$, and so the system becomes conditionally stable when $m_a = m_b$, which is equal to 1.1 kg. This prediction is found to be closely approximated in the simulations.

4.2. Integrated force feedback

Fig. 8(a) shows the frequency response of the plant from actuator force input to the integrated force output for the arrangement shown in Fig. 5 with an added mass of 0.5 kg on the equipment, and the Nyquist plot is shown in Fig. 8(b).

The resonance frequencies are the same as for velocity feedback, as shown in Fig. 6(a), but the frequency of the antiresonance, which is still accurately predicted by Eq. (35), is now much closer to the equipment resonance, as also shown in the root locus diagram in Fig. 8(c). The performance of the closed loop system is shown in Fig. 8(d), where again the feedback gain has been adjusted so that the phase margin is 120°. Comparing the performance with integrated force feedback with the corresponding result for absolute velocity feedback, Fig. 6(d), it can be seen that for the same phase margin (120°) the integrated force feedback strategy gives greater control of the first, mount-dominated, resonance, but lower levels of attenuation of the second, equipment-dominated, resonance.

When the added mass on the equipment is increased to 3.5 kg, the integrated force plant frequency response is as shown in Fig. 9(a). The resonance frequencies are the same as those for velocity feedback, in Fig. 7(a), but now the antiresonance frequency, predicted from Eq. (35) to be 16.3 Hz, occurs *between* the two resonances and so the phase lag does not accumulate and remains almost within $\pm 90°$, as seen on the Nyquist plot in Fig. 9(b).

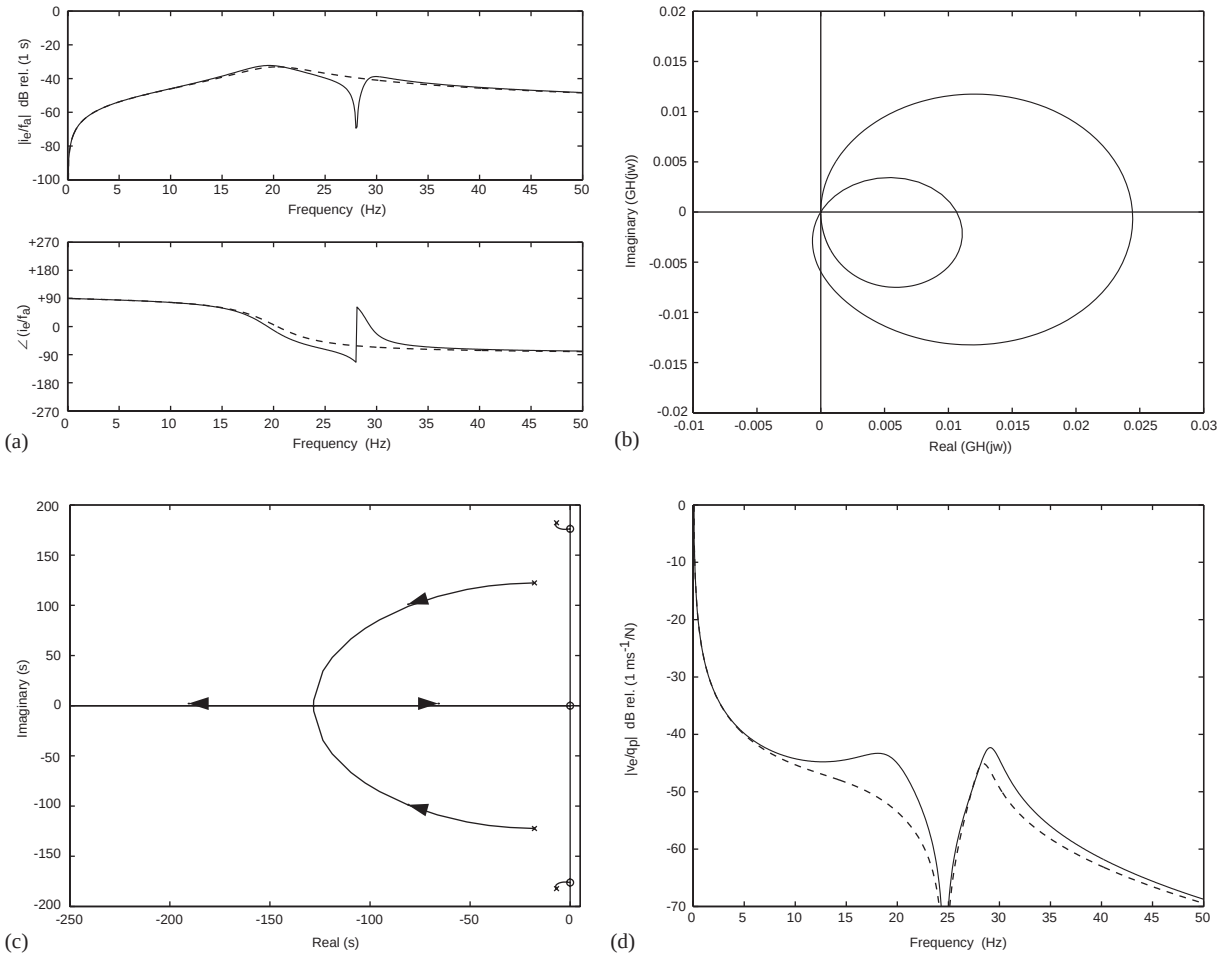

Fig. 8. (a) Frequency response of the plant from actuator force to integrated equipment force for the system shown in Fig. 5 with $m_a = 0.5\,\text{kg}$ (solid line) and with the equipment dynamics suppressed by setting $k_a = \infty$ (dashed line). (b) Nyquist plot of the plant response from actuator force to integrated equipment force for the system shown in Fig. 5 with $m_a = 0.5\,\text{kg}$. (c) Root locus diagram for the feedback system with the plant response from actuator force to integrated equipment force for the system shown in Fig. 5 with $m_a = 0.5\,\text{kg}$. (d) Open and closed loop responses from a force on the base structure to the equipment velocity for the system shown in Fig. 5 with integrated force feedback and $m_a = 0.5\,\text{kg}$.

This antiresonance is again undamped, and appears on the imaginary axis of the root locus diagram shown in Fig. 9(c). The performance is shown in Fig. 9(d) with the feedback gain again adjusted so that the phase margin is 120°, where attenuation of both resonances is seen. This example clearly illustrates the fact that integrated force feedback can be a more stable strategy than absolute velocity feedback under the rather extreme conditions where the attached mass is considerably greater than the mass of either the main equipment structure or the base and the base structure is unattached to the ground [6].

In the following section an example is considered in which the base structure is grounded but is also flexible, so that its dynamics will only be mass-controlled over certain ranges of frequency.

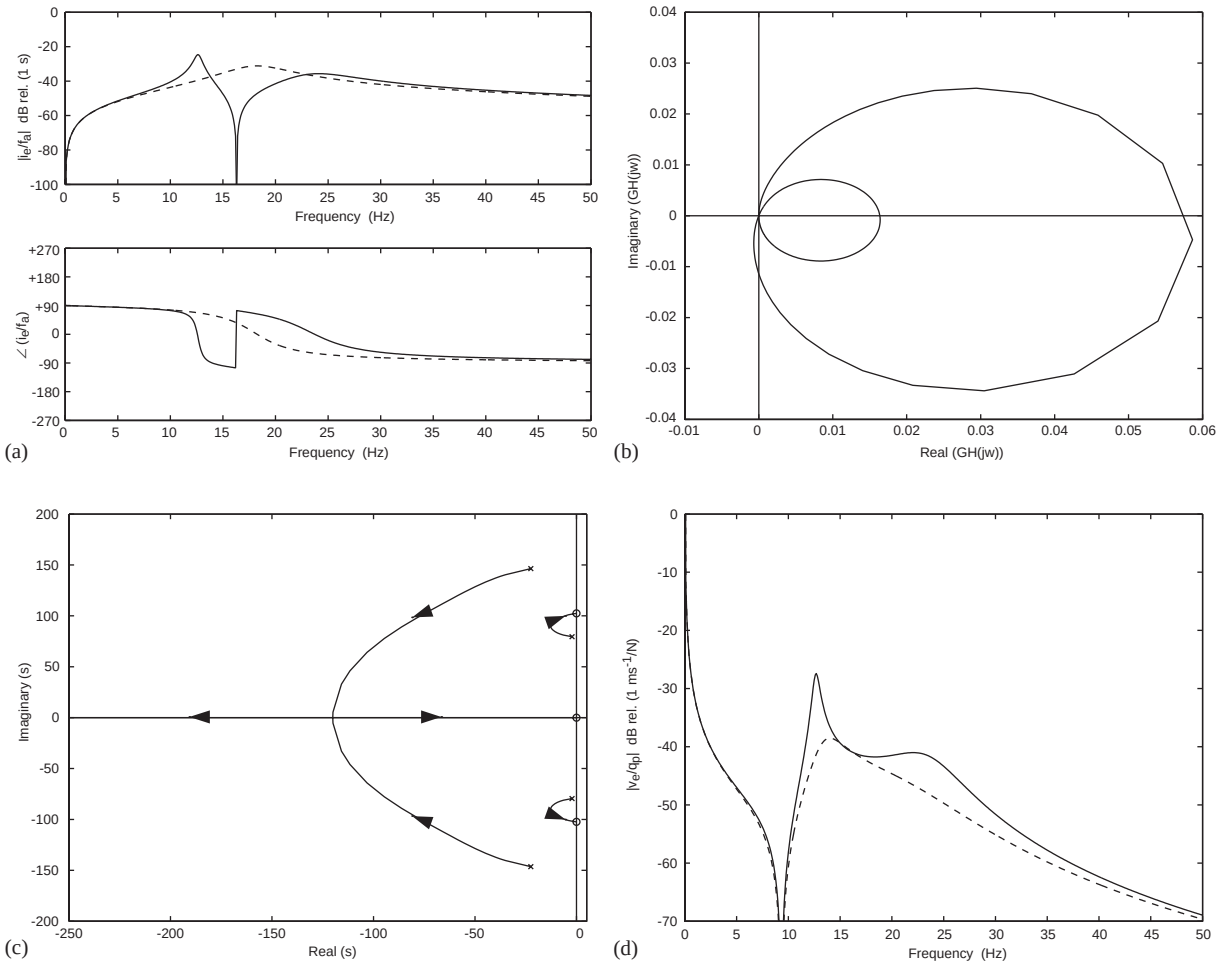

Fig. 9. (a) Frequency response of the plant from actuator force to integrated equipment force for the system shown in Fig. 5 with $m_a = 3.5\,\text{kg}$ (solid line) and with the equipment dynamics suppressed by setting $k_a = \infty$ (dashed line). (b) Nyquist plot of the plant response from actuator force to integrated equipment force for the system shown in Fig. 5 with $m_a = 3.5\,\text{kg}$. (c) Root locus diagram for the feedback system with the plant response from actuator force to integrated equipment force for the system shown in Fig. 5 with $m_a = 3.5\,\text{kg}$. (d) Open and closed loop responses from a force on the base structure to the equipment velocity for the system shown in Fig. 5 with integrated force feedback and $m_a = 3.5\,\text{kg}$.

5. Case of a flexible base structure

5.1. The isolation system

In this section we consider the case of an isolation system in which both the equipment structure and the base structure are flexible. The mechanical arrangement is illustrated in Fig. 10 and described fully by Huang et al. [13]. It consists of a flexible steel base plate $700 \times 500 \times 2\,\text{mm}$ thick,

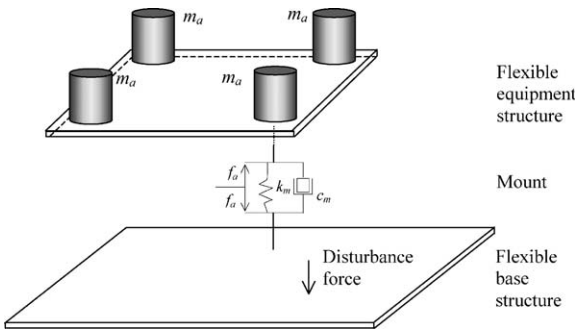

Fig. 10. Physical arrangement of an isolation system in which the equipment structure is a flexible plate attached to a base plate, which is clamped on two sides, by four mounts.

clamped on the two longer sides, which supports a flexible equipment structure consisting of a 300 mm × 160 mm × 3.2 mm thick aluminium plate on which 4 electromagnetic actuators are mounted, each of mass 0.91 kg. The equipment structure is normally supported by four mounts underneath the actuators, each of which has a stiffness, k_m, of 1.2×10^4 N m^{-1} and damping, c_m, of 11.5 N s m^{-1}. In the experimental system described by Huang et al. [13], the control forces are transmitted from the actuators to the base structure through the hollow passive mounts.

We will consider a single-channel active isolation system here, implemented at only one mount location. The control forces are again modelled as being in parallel and collocated with the mount, as shown in Fig. 10. The theoretical model described by Huang et al. [13] has been used to predict the input mobility of the equipment plate at this mount position, as shown in Fig. 11(a), complete with the mass loading effects of the electromagnetic shakers. At low frequencies the mobility falls with frequency and has a phase of -90° since it is determined by the mass of the equipment structure. The first flexural resonance of the equipment structure, a torsional mode, occurs at about 54 Hz and this creates a resonance in the mobility response at this frequency and an antiresonance at about 47 Hz, because of the interference between the rigid body mode and the first flexible mode. Between about 47 and 54 Hz the equipment mobility rises with frequency and has a phase shift of $+90^\circ$ and is thus stiffness-dominated. The dynamic stiffness of the equipment structure is much larger than that of the mount over almost all of this frequency range. Above 54 Hz the mobility again becomes mass-dominated until about 140 Hz, where the second flexible mode of the equipment structure occurs.

The input mobility of the base structure at the mounting position is shown in Fig. 11(b). At low frequencies this rises with frequency and has a phase of $+90^\circ$ because it is stiffness-dominated, as expected for a plate clamped on two sides to a rigid base. The first flexural resonance of the base plate occurs at about 40 Hz and between this frequency and the frequency of the next antiresonance, at about 48 Hz, the mobility falls with frequency and has a phase shift of -90°, and is thus mass-dominated. Further flexural modes of the base plate occur at about 60 and 140 Hz with alternating stiffness-controlled and mass-controlled behaviour in between.

It was originally coincidental that in these simulations the base structure should be mass-controlled over part of the frequency range in which the equipment structure is stiffness-controlled. It does, however, provide worst-case conditions from the point of view of the stability

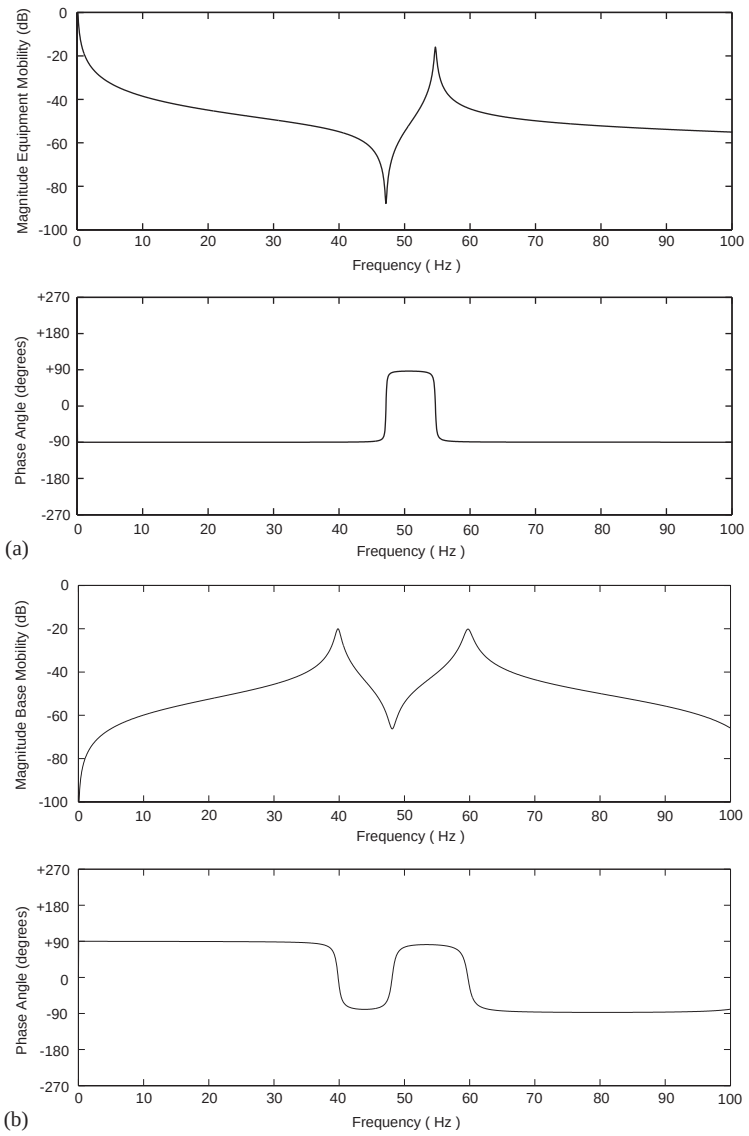

Fig. 11. The input mobility of the equipment structure (a) and the base structure (b) shown in Fig. 10 at one of the mounting points.

of an absolute velocity feedback system, as discussed in Section 2, and may thus be seen to be a challenging case to consider.

5.2. *Absolute velocity feedback*

Fig. 12(a) shows the frequency response of the plant, from reactive force input to absolute equipment velocity output for the isolation system described above, and Fig. 12(b) shows the corresponding Nyquist plot, indicating the system is unconditionally stable.

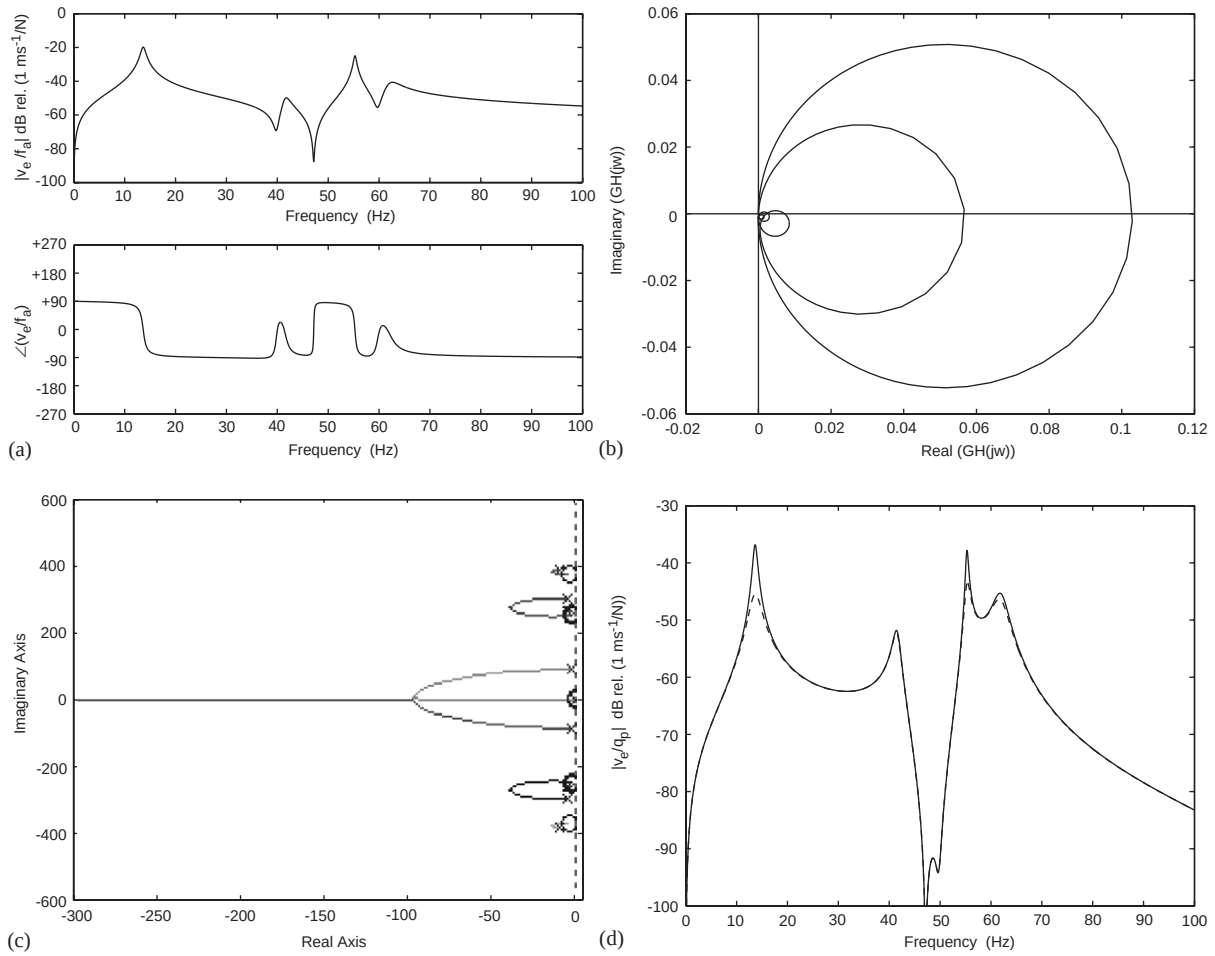

Fig. 12. (a) Frequency response of the plant response from actuator force to absolute equipment velocity for the isolation system with a flexible base structure, as shown in Fig. 10. (b) Nyquist plot of the plant response. (c) Root locus plot of the velocity feedback diagram. (d) Open (thick line) and closed (thin line) loop equipment velocity responses.

Returning to the conditions discussed at the end of Section 2, which are necessary for a conditionally stable system, we see from Figs. 11(a) and (b) that two of these three conditions are satisfied from about 47 Hz when the equipment becomes stiffness controlled, to 48 Hz, above which the base is not mass-controlled. The third condition can be evaluated at the worst-case frequency of 47 Hz, at which the effective mass of the base, m_b, is about 2.5 kg. The dynamic stiffness of the equipment is significantly higher than that of the mount at this frequency so the total stiffness, k_t, is approximately equal to k_m, which is $12 \times 10^4\,\mathrm{N\,m^{-1}}$. In this case the stability parameter defined in Section 2 is thus equal to

$$\frac{k_t}{\omega^2 m_b} = 0.05 \quad \text{at } 47\,\text{Hz}, \tag{45}$$

and the system is predicted to be unconditionally stable. The simple rules derived in Section 2 for judging the stability of a velocity-feedback isolation system thus do a good job of predicting the behaviour of the controller even in this complicated structure.

Fig. 12(c) shows the root locus diagram for this system, which has pairs of poles corresponding to the resonances at 14, 42 and 54 Hz, and an additional pole with a closely spaced zero at about 60 Hz. Each of the root loci from the open loop poles to the open loop zeros move to the left in this diagram, indicating greater damping, except the pole-zero pair at about 60 Hz, for which the root locus initially moves slightly to the right, to an extent which is difficult to observe in Fig. 12(c), but does not cross the real axis again, confirming that the system is unconditionally stable.

This isolation system can become conditionally stable, however, if some of its characteristics are changed. If, for example, the stiffness of the mount, and hence k_t in Eq. (45) was increased by a factor of 20, the stability parameter would become greater than unity and the system would be conditionally stable. More subtly, however, if the thickness of the equipment structure is reduced from 3.2 to 2.9 mm, its first flexural resonance then occurs at 47 Hz instead of 54 Hz and the equipment structure is stiffness-controlled from 41 to 47 Hz. The effective mass of the base structure at 41 Hz is only about 0.2 kg and $k_t/\omega^2 m_b$ is then about 1.8 at this frequency, indicating that the system is only conditionally stable. The magnitude of the plant response is, however, very small at 41 Hz, because $Y_e(j\omega)$ has a very small magnitude at this frequency, and so the system would not become unstable until the feedback gains were extremely high.

Fig. 12(d) shows the equipment velocity due to a primary force acting on the base plate before control (solid line) and with velocity feedback control (dashed line), where the gain has again been adjusted to give a phase margin of 120°. About 10 dB of attenuation is achieved at the first, mounted equipment, resonance at about 14 Hz and about 6 dB of attenuation is achieved at the first base resonance, at about 54 Hz.

The isolation system shown in Fig. 10 has four mounts, but in this section control has only been considered for a single mount. The reductions in equipment velocity above this mount, as shown in Fig. 12(d), can thus be accompanied by increases in the equipment velocity above the other mounts, as the single channel control system acts to pin the equipment at one point. Global control of the equipment's vibration can only be achieved by actively controlling each of the four mounts [13].

5.3. Integrated force feedback

Fig. 13(a) shows the magnitude and phase of the frequency response from actuator input to integrated equipment force output for the isolation system shown in Figs. 10, and 13(b) and (c) shows the corresponding Nyquist and root locus plot. The magnitudes of the peak due to the equipment's internal resonance, at about 54 Hz, is now much smaller than that due to the main isolator resonance, at about 12 Hz.

Fig. 13(d) shows the open and closed loop equipment velocity response to a unit primary force on the base plate, again arranged to have a 120° phase margin. The attenuation at the mounted equipment resonance is again about 10 dB, but the attenuation at the equipment resonance is now very small.

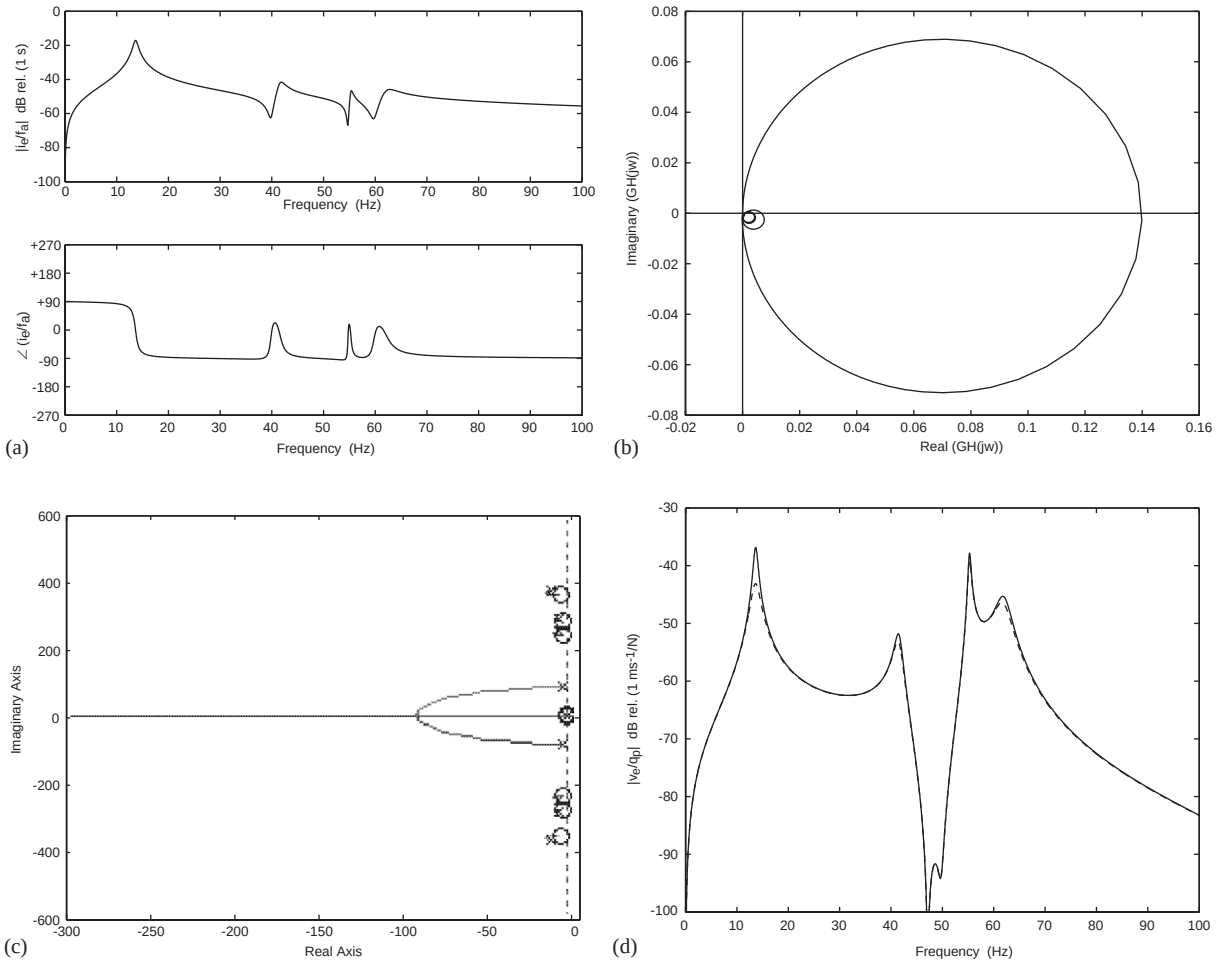

Fig. 13. (a) Frequency response of the plant response from actuator force to integrated force for the isolation system with a flexible base structure, as shown in Fig. 10. (b) Nyquist plot of the plant response. (c) Root locus plot of the velocity feedback diagram. (d) Open (thick line) and closed (thin line) loop equipment velocity responses.

6. Summary and conclusions

A general analysis has been presented of the plant response in an active isolation system with either absolute velocity feedback or integrated force feedback, in terms of the mechanical impedance of the mount and the mechanical mobilities of the equipment structure and the base structure.

When the reciprocal of the plant frequency responses is considered, it can be seen that for integrated force feedback, the plant's phase response is restricted to be between -180° and 90°. In the absence of actuator and sensor dynamics, this feedback loop is thus unconditionally stable.

When a similar analysis is performed for absolute velocity feedback, the limits on the phase of the plant's frequency response are increased, to be between -180° and 270°. This feedback

control system is thus, in general, only conditionally stable. The frequency domain analysis can, however, also be used to determine the specific conditions under which the plant's phase shift becomes greater than 180° and thus causes stability problems. These are three-fold: first the base must be mass-dominated, second the equipment must be stiffness-dominated and third the ratio of the base mobility to the mount and equipment mobility must have a modulus which is greater than unity.

In the special case in which the base is rigid, the phase of the plant's frequency response for integrated force feedback is still $-180°$ to 90°, but for absolute velocity feedback, the phase is now restricted to $-90°$ to $+90°$. This is because the plant response is equal to a passive input mobility function and so the velocity feedback system is not only unconditionally stable but is also very robust under these conditions.

Numerical simulations have been used to illustrate the frequency response, Nyquist plot and root locus plot for the particular case of an active isolation system with a rigid base and a dynamic equipment structure, modelled as a two degree of freedom system. Both absolute velocity feedback and integrated force feedback give a similar reduction in the transmissibility at the natural frequency of the isolation system, but absolute velocity feedback also provides good reductions at the natural frequency of the internal equipment resonance. If the equipment is rigid but the base is flexible, both feedback strategies are seen to be equivalent.

When the base structure is assumed to be a mass, however, the absolute velocity feedback system becomes only conditionally stable when the natural frequency of the internal equipment resonance falls below the natural frequency of the isolation system. If the natural frequency of the dynamic equipment structure is above the natural frequency of the isolation system, on the other hand, the absolute velocity feedback system is unconditionally stable and again provides a greater degree of attenuation at the natural frequency of the equipment than integrated force feedback.

Finally, the case is considered in which both the equipment structure and the base structure are flexible. Although it is then possible for the base dynamics to be mass-dominated and the equipment dynamics to be stiffness-dominated at the same frequency, absolute velocity feedback still appears to be a stable strategy until the feedback gain is much higher than is required for good attenuation. Absolute velocity feedback again has the advantage of attenuating not just the main resonance of the isolation system, but also resonances due to the flexibility of the equipment.

Acknowledgements

This work was performed under EPSRC Grant Number GR/M 24424.

References

[1] C.M. Harris, *Shock and Vibration Handbook*, 3rd Edition, McGraw Hill, NewYork, 1998.

[2] D. Karnopp, Active and semi-active vibration isolation, *American Society of Mechanical Engineers, Journal of Mechanical Design* 177 (1995) 177–185.

[3] S.J. Elliott, M. Serrand, P. Gardonio, Feedback stability limits for active isolation systems with reactive and inertial actuators, *American Society of Mechanical Engineers, Journal of Vibration and Acoustics* 123 (2001) 250–261.

[4] A.B. Watters, R.B. Coleman, G.L. Duckworth, E.F. Berkman, A perspective on active machinery isolation, *Proceedings of the 27th Conference on Decision and Control*, Austin, TX, 1988, pp. 2033–2038.
[5] A. Preumont, *Vibration Control of Structures: An Introduction*, 2nd Edition, Kluwer, Dordrecht, 2002.
[6] A. Preumont, A. François, F. Bossens, A. Abu-Hanieh, Force feedback versus acceleration feedback in active vibration isolation, *Journal of Sound and Vibration* 257 (4) (2002) 605–613.
[7] G.M. Blackwood, A.H. Von Flotow, Active control for vibration isolation despite resonant structural dynamics: a trade study of sensors, actuators and configurations *Proceedings of the 2nd Conference on Recent Advances in Active Control of Sound and Vibration*, Virginia Polytechnic Institute, Blacksburg, VA, 1993.
[8] M. Serrand, Direct Velocity Feedback Control of Equipment Velocity, MPhil Thesis, University of Southampton, Southampton, 2000.
[9] D. Sciulli, D.J. Inman, Isolation design for a flexible system, *Journal of Sound and Vibration* 216 (2) (1998) 251–267.
[10] G.F. Franklin, J.D. Powell, A. Emami-Naeini, *Feedback Control of Dynamic Systems*, 3rd Edition, Addison-Wesley, Reading, MA, 1994.
[11] M.Z. Ren, K. Seto, F. Doi, Feedback structure-borne sound control of a flexible plate with an electromagnetic actuator: the phase lag problem, *Journal of Sound and Vibration* 205 (1) (1997) 57–80.
[12] M.J. Brennan, K.A. Ananthaganeshan, S.J. Elliott, Low and high frequency instabilities in feedback control of vibrating single-degree-of-freedom systems, P. Gardonio, B. Rafaely (Eds.) *Proceedings of ACTIVE 2002*, Vol. 2, Southampton, 2002, pp. 1317–1326.
[13] X. Huang, S.J. Elliott, M.J. Brennan, Active vibration isolation of a flexible equipment structure on a flexible base, ISVR Technical Memorandum No. 879, 2001.